Hindawi Publishing Corporation
Advances in Condensed Matter Physics
Volume 2015, Article ID 496739, 6 pages
http://dx.doi.org/10.1155/2015/496739

Research Article

Reduction of Lattice Thermal Conductivity in PbTe Induced by Artificially Generated Pores

Jae-Yeol Hwang,[1] Eun Sung Kim,[1] Syed Waqar Hasan,[2] Soon-Mok Choi,[3] Kyu Hyoung Lee,[4] and Sung Wng Kim[2]

[1]*Center for Integrated Nanostructure Physics, Institute for Basic Science (IBS), Sungkyunkwan University, Suwon 440-746, Republic of Korea*
[2]*Department of Energy Science, Sungkyunkwan University, Suwon 440-746, Republic of Korea*
[3]*School of Energy, Materials and Chemical Engineering, Korea University of Technology and Education, Cheonan 330-708, Republic of Korea*
[4]*Department of Nano Applied Engineering, Kangwon National University, Chuncheon 200-701, Republic of Korea*

Correspondence should be addressed to Kyu Hyoung Lee; khlee2014@kangwon.ac.kr and Sung Wng Kim; kimsungwng@skku.edu

Received 24 November 2014; Revised 25 February 2015; Accepted 25 February 2015

Academic Editor: Ram N. P. Choudhary

Highly dense pore structure was generated by simple sequential routes using NaCl and PVA as porogens in conventional PbTe thermoelectric materials, and the effect of pores on thermal transport properties was investigated. Compared with the pristine PbTe, the lattice thermal conductivity values of pore-generated PbTe polycrystalline bulks were significantly reduced due to the enhanced phonon scattering by mismatched phonon modes in the presence of pores (200 nm–2 μm) in the PbTe matrix. We obtained extremely low lattice thermal conductivity (~0.56 W m^{-1} K^{-1} at 773 K) in pore-embedded PbTe bulk after sonication for the elimination of NaCl residue.

1. Introduction

Thermal energy can be directly converted into electrical energy and vice versa through the flow of charge carriers in solid-state without any moving parts using thermoelectric (TE) materials [1, 2]; thus TE is focused as a key technology for renewable energy harvesting and solid-state refrigeration. Since the efficiency of TE device is directly determined by the performance of TE materials (ZT), which is defined as $ZT = S^2\sigma T/\kappa$, where S is the Seebeck coefficient, σ is the electrical conductivity, and κ is the thermal conductivity at a given absolute temperature T, researches have been mainly concentrated on discovering new concepts as well as experimental approaches to enhance ZT. Breaking the trade-off between σ and κ by reducing the lattice thermal conductivity (κ_{latt}) is one of the most effective approaches due to the relative easiness of controlling κ_{latt} without significantly affecting the carrier transport. In conventional TE materials such as Bi_2Te_3, PbTe, and SiGe, the perturbations of structural arrangements for enhancing phonon scattering through nanostructuring and/or solid-solution alloying have been shown to be one of the effective ways to minimizing κ_{latt} [3–8]. Recent experimental and theoretical results confirm that reduced κ_{latt} can be attained by the following mechanisms: alloy scattering [3–6], resonant scattering [9–13], anharmonic scattering [14], and interface scattering of phonons [15–17] or their combination.

Noninvasive formation of phonon scattering centers is another effective way to generate effective phonon scattering without altering the framework of TE materials and introducing other elements. One promising approach is the formation of nanoscale pore structure since such defect can be effective phonon scattering centers without sacrificing electronic transport properties (S and σ). How to control the dimension as well as distribution of pores is crucial to determine the frequency dependence of scattering mechanism for heat-carrying phonons [7–9]. Practically, it is important to make randomly distributed pores in the TE matrix through

simple and cost-effective routes. Here we report the simple and scalable technique for generation of highly dense pore structure by using cost-effective porogens (NaCl and PVA) in PbTe compounds. We investigated the relation between pore structure and thermal transport properties considering structural features of pore-embedded PbTe.

2. Experimental

Crystal ingots of PbTe were prepared by conventional melting technique by the use of high-purity elemental Pb (>99.99%, Sigma-Aldrich) and Te (>99.999%, 5 N Plus) as starting materials. Pb and Te granules were weighed with a stoichiometric ratio of the elements and sealed in an evacuated fused silica tube 12 mm in diameter. The tube was heated to 1323 K in a box furnace for 10 h to make congruent melting and then slowly cooled down to room temperature. The ingots were ground into powders using ball mill, and mixed powders of PbTe and porogens (NaCl and PVA) were formed by a simple mixing of PbTe and porogens powders using high-energy ball mill. Inorganic and organic materials such as 3 wt.% (equal to 10 vol.%) of NaCl (Sigma-Aldrich) and 2 wt.% (equal to 11 vol.%) of polyvinyl alcohol (PVA, chemical formula: $[CH_2CH(OH)]_n$, Sigma-Aldrich) were used as porogens. These materials were chosen because of the easiness of handling, abundance, and good solubility in water. The huge difference in water solubility between PbTe and porogens enables the formation of pores without deteriorating PbTe matrix. Then disk-shaped polycrystalline bulk samples of 10 mm in diameter and 3 mm in thickness were prepared using spark plasma sintering (SPS) technique under dynamic vacuum and with the application of 80 MPa of uniaxial pressure at 573 K for 3 min. For convenience, NaCl- and PVA-embedded PbTe samples consolidated by SPS denote PbTe + NaCl and PbTe + PVA, respectively. The relative density of the pristine PbTe bulk sample was about 97%, while those of PbTe + NaCl and PbTe + PVA were slightly higher (~98%). The phases of PbTe powders were analyzed by powder X-ray diffraction analysis using an X-ray diffractometer (XRD, Rigaku Smartlab) equipped with Cu Kα radiation (λ = 1.5418 Å). Microstructural and morphological changes of compacted samples were investigated by scanning electron microscopy (SEM, JEOL JSM-7600F). The σ values from 300 K to 773 K were measured using a ZEM-3 system (ULVAC-RICO, Japan). The κ values ($\kappa = \rho_s C_p \lambda$) were calculated from measurements taken separately: sample density (ρ_s), heat capacity (C_p), and thermal diffusivity (λ) measured under vacuum by laser-flash method (TC-9000, ULVAC, Japan), in which C_p was used as the constant value of 0.155 J g^{-1} K^{-1} estimated from the Dulong-Petit fitting using low temperature C_p data. All measured data, which were acquired at the same dimension and configuration, are obtained within the experimental error about 5%.

3. Results and Discussion

We fabricated the pore-embedded PbTe polycrystalline bulks and evaluated their electronic and thermal transport properties to clarify the effects of pore structure on the phonon scattering behavior. Figures 1(a), 1(b), and 1(d) show the X-ray diffraction (XRD) patterns for SPS compacted PbTe, PbTe + NaCl, and PbTe + PVA bulk samples, respectively. For PbTe + NaCl sample, the peak for NaCl (2 0 0) is clearly seen, indicating that porogen materials remained in the PbTe matrix even after SPS process. In order to remove the porogen materials, PbTe + NaCl and PbTe + PVA bulk samples were sonicated in water. The residues of porogen materials were eliminated by 30 min sonication in the preheated 60°C deionized water owing to the high water solubility of NaCl and PVA. No other peaks corresponding to porogen materials are detected after sonication process (Figures 1(c) and 1(e)). No differences in peak shift and lattice parameter were observed in XRD analysis (Figure 1) for PbTe, PbTe + NaCl, and PbTe + PVA samples regardless of sonication. Therefore, we consider that there is no considerable chemical reaction, such as substitutional doping of porogen or the formation of secondary phase, between host material and porogen in these samples. Calculated lattice parameters from XRD patterns for pristine PbTe and pore-embedded PbTe samples were $a = b = c = 6.460(4)$ Å. The elimination of porogen residues and formation of pore structure are confirmed by SEM analysis. Figure 2(a) shows simplified schematics of the route for pore generation using porogens (NaCl and PVA). Firstly, porogens were uniformly mixed with pulverized PbTe powders by high-energy ball milling. Secondly, porogens were embedded in bulk PbTe during the pressure-induced sintering process such as SPS. Finally, residues of porogen materials were removed by sonication in water. Figures 2(b) and 2(d) show the SEM images of fractured surfaced SPS compacted PbTe + PVA and PbTe + NaCl samples. There was no pore-like structure suggesting added porogen materials are embedded in PbTe matrix; thus the relative densities of those were relatively high (~98%), while highly dense nano- and microscale pores (200 nm–2 μm) are clearly seen after sonication (Figures 2(c) and 2(e)). The relative densities of sonicated PbTe + PVA and PbTe + NaCl bulks were reduced

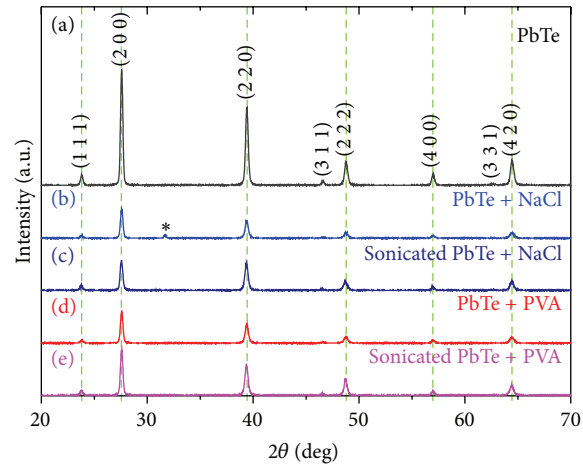

Figure 1: X-ray diffraction patterns of (a) PbTe PbTe + NaCl (b) before and (c) after sonication, and (d) PbTe + PVA (d) before and (e) after sonication. Asterisk (∗) represents NaCl phase and green dotted lines are guidelines for peak positions.

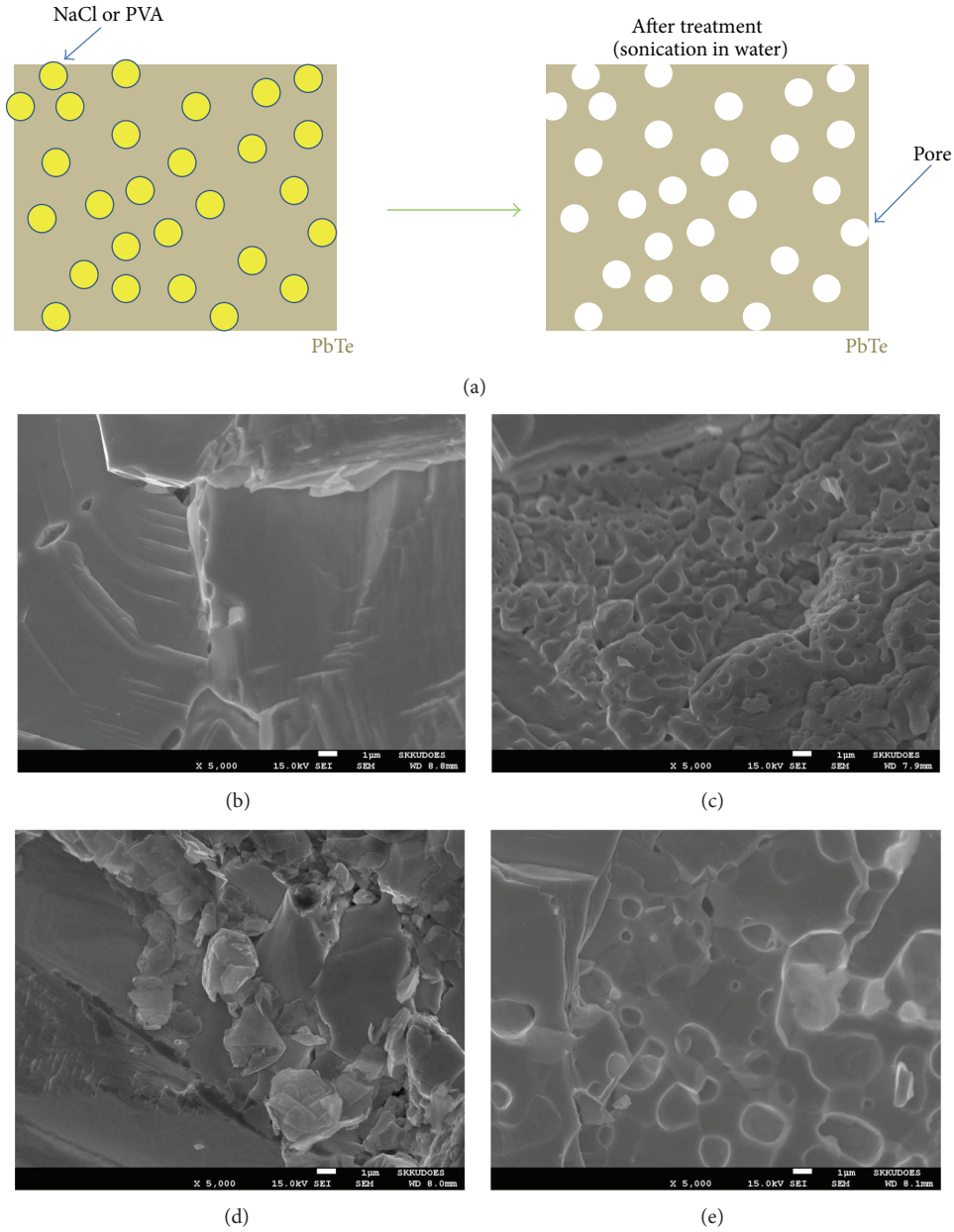

FIGURE 2: (a) Schematics of pore generation in the PbTe host matrix using PVA or NaCl. Scanning electron microscopy images of the fractured surfaces for (b) before and (c) after sonication for PbTe + PVA samples and (d) before and (e) after sonication for PbTe + NaCl, respectively.

to the value about 96% and 95%, respectively. This indicates that pores were generated with the porosity of ~7.3% in both of the sonicated porogen-embedded samples.

Pore structure formation can also be confirmed in κ and σ data. Figure 3(a) shows the temperature dependence of evaluated κ values for PbTe + NaCl, PbTe + PVA, sonicated PbTe + NaCl, and sonicated PbTe + PVA bulk samples. That of the pristine PbTe sample is shown for comparison. As shown in Figure 3(a), the κ values of PbTe + NaCl and PbTe + PVA were lower than those of pristine PbTe over whole measured temperature range despite restricted pore generation (Figures 2(b) and 2(d)). It could be understood from the expectation that porogens act as scattering center for heat-carrying phonons. Further, it should be noted that κ values of PbTe + NaCl and PbTe + PVA were significantly reduced by sonication. To clarify this thermal transport behavior, we measured σ (inset of Figure 3(b)) and calculated κ_{latt} using the following equation: $\kappa_{\text{total}} = \kappa_{\text{latt}} + \kappa_{\text{elec}}$, where the electronic contribution (κ_{elec}) is estimated from the Wiedemann-Franz law, $\kappa_{\text{elec}} = L_0 T\sigma$ with the Lorenz number, $L_0 = 2.45 \times 10^{-8}$ W ohm K^{-2} [18]. Compared with PbTe, κ_{latt} values of PbTe + NaCl and PbTe + PVA were decreased especially at higher temperatures. The κ_{latt} values of them were rather reduced by about 20% at 773 K despite limited

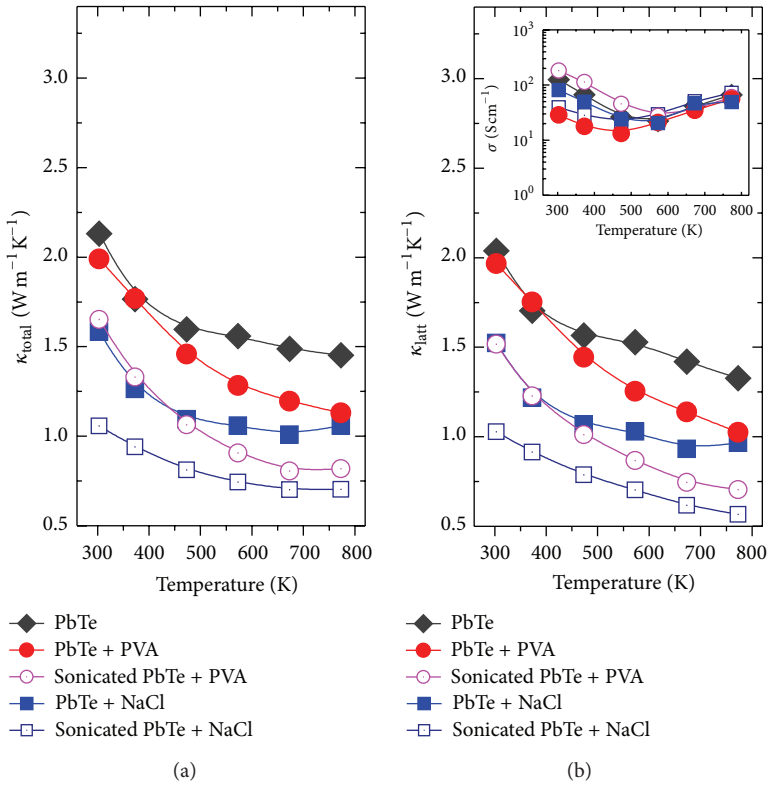

FIGURE 3: (a) Total and (b) lattice thermal conductivities as a function of temperature for PbTe and PVA- and NaCl-embedded PbTe samples before and after sonication, respectively. The inset shows the temperature dependence of electrical conductivity for all samples.

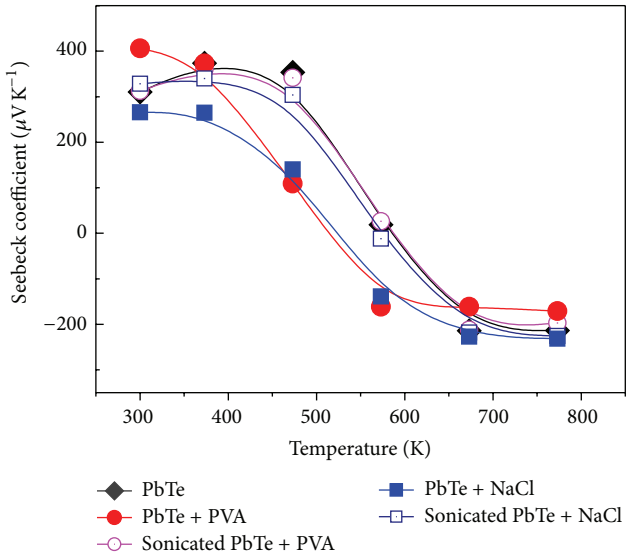

FIGURE 4: Seebeck coefficient values as a function of temperature for PbTe and PVA- and NaCl-embedded PbTe samples before and after sonication, respectively.

pore structure (Figure 3(b)). This is considered to be related with the heterointerface between PbTe matrix and porogens and low κ values of NaCl (~0.1 W m^{-1} K^{-1} at 300 K) and PVA (~0.2 W m^{-1} K^{-1} at 300 K) compared to that of PbTe (~2.04 W m^{-1} K^{-1} at 303 K). On the other hand, extremely low values of κ_{latt} 0.56 W m^{-1} K^{-1} and 0.70 W m^{-1} K^{-1} at 773 K were obtained in sonicated PbTe + NaCl and PbTe + PVA, respectively, due to the intensified phonon scattering in the presence of pores (Figures 2(c) and 2(e)). In comparison with the values of pristine PbTe (κ_{latt} ~ 2.04 W m^{-1} K^{-1} at 303 K and ~1.32 W m^{-1} K^{-1} at 773 K), κ_{latt} decreased by 50% (1.02 W m^{-1} K^{-1}) at 303 K and by more than 58% (0.56 W m^{-1} K^{-1}) at 773 K in sonicated PbTe + NaCl. These indicate that the strong phonon scattering was induced in the presence of randomly distributed pores due to the reduction in the channels for phonon transport path and the increased phonon scattering at the pore surfaces by mismatched phonon modes [19]. In Figure 4, Seebeck coefficient values were changed by introducing porogens into the PbTe host matrix due to the differences in density as well as in physical properties between PbTe and porogens, which might produce composite-like effect. However, after sonication that induces the formations of pores in the PbTe host matrix by removing porogens, Seebeck coefficient values of pore-embedded PbTe samples as a function of temperature were similar to those of pristine PbTe. This indicates that the pore generation by demonstrated method here does not considerably affect the thermopower nature of PbTe host matrix. Initially, electrical conductivity values of PbTe + PVA sample are lower than those of pristine PbTe in the measured temperature range. However, after sonication, electrical conductivity was drastically increased

in the temperature range from 300 to 600 K. This might be related to the chemical decomposition of PVA that is dissolved in water and actively removed during sonication, leading to the generation of pores. Probably, some linkages of PVA (mainly carbon residue) remained at the grain boundaries of PbTe host matrix or at the interface between pores and matrix, providing the conducting path for low-energy carriers. This might keep the thermopower nature of PbTe matrix in the sonicated PbTe + PVA sample, enhancing the electrical conductivity. Theoretically, it was predicted that κ_{latt} reduction depends not only on the density of pore (porosity) but also on the size of pore and is much stronger if the separation between pores is comparably smaller than the mean free path of phonon and the size of pore is getting smaller [19]. Although the optimization of processing technique for the generation of monodispersed nanoscale pores with less than 50 nm in diameter is highly required to realize both strong scattering of heat-carrying phonon and maintaining electronic transport properties (phonon glass electron crystal), it was experimentally demonstrated that κ_{latt} could be significantly reduced by the formation of pore structure. An additional study for the correlation between pore size (as well as porosity) and thermal transport properties will be reported in elsewhere.

4. Conclusions

In this paper, we successfully fabricated the pore structure in PbTe matrix without any secondary phase through simple sequential routes of mixing, consolidation, and sonication using NaCl and PVA as porogens. By introducing pores in the PbTe matrix, the lattice thermal conductivity was significantly decreased by 58% for pore-embedded PbTe by NaCl, which originated from intensified phonon scattering by the reduction in the propagation paths for phonon transport in the presence of randomly distributed pores. We expect that this concept can be applied to most of thermoelectric materials to enhance thermoelectric performance by reduction of the lattice thermal conductivity since this methodology cannot alter crystal structure and chemical compositions of host thermoelectric materials by generating pores inside the grains and/or at the grain boundaries.

Conflict of Interests

The authors declare that there is no conflict of interests regarding the publication of this paper.

Acknowledgments

This work was supported by Human Resources Development Program (no. 20124010203270) of Korea Institute of Energy Technology Evaluation and Planning (KETEP) grant funded by Korea Government Ministry of Trade, Industry and Energy and R&D Convergence Program (Grant B551179-12-02-00) of MSIP (Ministry of Science, ICT and Future Planning) and NST (National Research Council of Science and Technology) of Republic of Korea.

References

[1] F. J. Disalvo, "Thermoelectric cooling and power generation," *Science*, vol. 285, no. 5428, pp. 703–706, 1999.

[2] G. J. Snyder and E. S. Toberer, "Complex thermoelectric materials," *Nature Materials*, vol. 7, no. 2, pp. 105–114, 2008.

[3] H. J. Goldsmid, "Recent studies of bismuth telluride and its alloys," *Journal of Applied Physics*, vol. 32, no. 10, pp. 2198–2202, 1961.

[4] B. Abeles, "Lattice thermal conductivity of disordered semiconductor alloys at high temperatures," *Physical Review*, vol. 131, no. 5, pp. 1906–1911, 1963.

[5] W. M. Yim, E. V. Fitzke, and F. D. Rosi, "Thermoelectric properties of Bi_2Te_3-Sb_2Te_3-Sb_2Se_3 pseudo-ternary alloys in the temperature range 77 to 300°K," *Journal of Materials Science*, vol. 1, no. 1, pp. 52–65, 1966.

[6] C. Wood, "Materials for thermoelectric energy conversion," *Reports on Progress in Physics*, vol. 51, no. 4, pp. 459–539, 1988.

[7] B. Wölfing, C. Kloc, J. Teubner, and E. Bucher, "High performance thermoelectric Tl_9BiTe_6 with an extremely low thermal conductivity," *Physical Review Letters*, vol. 86, no. 19, pp. 4350–4353, 2001.

[8] K. Kurosaki, A. Kosuga, H. Muta, M. Uno, and S. Yamanaka, "Ag_9TlTe_5: a high-performance thermoelectric bulk material with extremely low thermal conductivity," *Applied Physics Letters*, vol. 87, no. 6, Article ID 061919, 2005.

[9] B. C. Sales, D. Mandrus, and R. K. Williams, "Filled skutterudite antimonides: a new class of thermoelectric materials," *Science*, vol. 272, no. 5266, pp. 1325–1328, 1996.

[10] V. Keppens, D. Mandrus, B. C. Sales et al., "Localized vibrational modes in metallic solids," *Nature*, vol. 395, no. 6705, pp. 876–878, 1998.

[11] J. Yang, W. Zhang, S. G. Bai, Z. Mei, and L. D. Chen, "Dual-frequency resonant phonon scattering in $Ba_xR_yCo_4Sb_{12}$ (R = La, Ce, and Sr)," *Applied Physics Letters*, vol. 90, no. 19, Article ID 192111, 2007.

[12] J. L. Cohn, G. S. Nolas, V. Fessatidis, T. H. Metcalf, and G. A. Slack, "Glass like heat conduction in high-mobility crystalline semiconductors," *Physical Review Letters*, vol. 82, no. 4, pp. 779–782, 1999.

[13] D. Y. Chung, T. Hogan, P. Brazis et al., "$CsBi_4Te_6$: a high-performance thermoelectric material for low- temperature applications," *Science*, vol. 287, no. 5455, pp. 1024–1027, 2000.

[14] O. Delaire, J. Ma, K. Marty et al., "Giant anharmonic phonon scattering in PbTe," *Nature Materials*, vol. 10, no. 8, pp. 614–619, 2011.

[15] W. J. Xie, X. F. Tang, Y. G. Yan, Q. J. Zhang, and T. M. Tritt, "Unique nanostructures and enhanced thermoelectric performance of melt-spun BiSbTe alloys," *Applied Physics Letters*, vol. 94, no. 10, Article ID 102111, 2009.

[16] W. K. Liebmann and E. A. Miller, "Preparation, phase–boundary energies, and thermoelectric properties of InSb–Sb eutectic alloys with ordered microstructures," *Journal of Applied Physics*, vol. 34, no. 9, pp. 2653–2659, 1963.

[17] A. I. Hochbaum, R. Chen, R. D. Delgado et al., "Enhanced thermoelectric performance of rough silicon nanowires," *Nature*, vol. 451, no. 7175, pp. 163–167, 2008.

[18] S. N. Girard, J. He, C. Li et al., "In situ nanostructure generation and evolution within a bulk thermoelectric material to reduce lattice thermal conductivity," *Nano Letters*, vol. 10, no. 8, pp. 2825–2831, 2010.

[19] J.-H. Lee, J. C. Grossman, J. Reed, and G. Galli, "Lattice thermal conductivity of nanoporous Si: molecular dynamics study," *Applied Physics Letters*, vol. 91, no. 22, Article ID 223110, 2007.